Austrian Journal of Earth Sciences | Volume 105/1 | 224 - 239 | Vienna | 2012

Palynology, biomarker assemblages and clay mineralogy of the Early Eocene Climate Optimum (EECO) in the transgressive Krappfeld succession (Eastern Alps, Austria)

Christa-Ch. HOFMANN[1)*], Richard PANCOST[2)], Franz OTTNER[3)], Hans EGGER[4)], Kyle TAYLOR[2)], Omar MOHAMED[5)] & Reinhard ZETTER[1)]

[1)] University of Vienna, Department of Palaeontology, Althanstr. 14, 1090 Vienna, Austria;

[2)] Organic Geochemistry Unit, Bristol Biogeochemistry Research Centre and The Cabot Institute, School of Chemistry, University of Bristol, Cantock's Close, BS8 1TS Bristol, UK;

[3)] University of Natural Resources and Applied Life Sciences, Gregor Mendel Straße 33, 1090 Vienna, Austria;

[4)] Geological Survey of Austria, Neulinggasse 38, 1030 Vienna, Austria;

[5)] El Minia University, Department of Geology, El Minia, Egypt;

[*)] Corresponding author, christa.hofmann@univie.ac.at

KEYWORDS

northwestern Tethys
Clay mineralogy
Eastern Alps
Early Eocene
Palynology
Tex

Abstract

Sediments of the Eocene Holzer Formation from the Pemberger quarry were analysed for palynomorphs, lipid biomarker distributions, and clay mineralogy. The palynoflora is rich in megathermal and mesothermal families and genera, but also contain abundant wind-derived pollen derived from temperate to mesothermal taxa. The co-existence of temperate to megathermal elements suggests a sub/tropical and seasonally controlled passat-like or monsoon-like climate, comparable with the extant forests of the zonoecotone I/II, an interpretation consistent with relatively high temperatures derived from soil bacterial glycerol dialkyl glycerol tetraether (GDGT) lipid distributions. The lithologies and palynomorph assemblages represent three different facies: (1) coal-bearing palm swamp characterized by Myricaceae, triporate pollen types, fern spores and several palm pollen types, (2) coastal near swamp with mangrove elements such as *Nypa*, *Avicennia* and *Ceriops*, and (3) shrubby back swamp dominated by Myricaceae, triporate pollen, fern spores and palm pollen types. All of these are consistent with a dominance of terrigenous lipids, including triterpenoids and leaf waxes, in all samples. Abundant kaolinite contents in all the sediment samples are consistent with the biomarker and pollen analyses, indicating long periods with deep weathering under a warm and humid climate.

1. Introduction

The early Eocene was characterized by a series of short-lived episodes (<200 ka) of global warming, superimposed on a long-term early Cenozoic warming trend (see Zachos et al., 2010 and Galeotti et al., 2010 for reviews). For the Paleocene-Eocene Thermal Maximum (PETM or ETM 1, ca. 56 Ma, around NP9 within Chron 24r, Westerhold et al., 2007) and the Eocene Thermal Maximum 2 (ETM 2, ca. 53.6 Ma, below NP10/NP11, Lourens et al. 2005; or within Chron 24r, Westerhold et al., 2007), the transient rise of global temperatures has been estimated to be 4 to 8° C (Kennett and Stott, 1991; Lourens et al., 2005). Smaller transient warming events might include event I (ca. 53.2 Ma) and event K (ca. 52.4 Ma) of Cramer et al. (2003), the latter probably corresponding to event X (Röhl et al., 2005, Agnini et al., 2009).

Although these transient hyperthermals are of much interest (e.g. Zachos et al., 2008), longer term climate change has also been the subject of much scrutiny. In particular, the Early Eocene Climatic Optimum (EECO, around NP12; Chron 23n to 22n, Westerhold et al., 2007), defined by a long-term minimum in global benthic foraminiferal $\delta^{18}O$ values, represents one of the highest global temperatures recorded in the past 70 million years (Zachos et al., 2001) and certainly the highest temperatures for a sustained interval in the Cenozoic. This unusually warm period began at about the same time (ca. 53 Ma) worldwide, whereas its termination between 51- 49 Ma varies considerably by region (e.g. Hollis et al., 2009). EECO sea surface temperatures (SST) derived from GDGT distributions for the western tropical and southwestern Pacific appear to have been as high as 34ºC and 30ºC, respectively, generally warmer than modern tropical seas (Pearson et al., 2007) and much warmer than modern high latitude seas (Hollis et al., 2009; Bijl et al., 2009). However, the fidelity of especially the high latitude sites has been challenged (Huber and Caballero, 2011) and temperature records from other settings are required.

Crucially, although abundant marine sections have allowed for past and ongoing analysis of Eocene SSTs, it is far more difficult to correlate Eocene continental macro- or microfloras with climatic events because of the lack of a precise stratigraphic framework (be it isotopic, magnetic or biostratigraphic) and the relatively episodic nature of the deposits. There are exceptions, such as the well dated tuffs within the Green River Formation in Wyoming that cover a time range from 53.5 to 48.5 Ma (Chrons 24n to 21r) and spans the whole EECO and probably the ETM2 (Smith et al., 2003). However, continental palaeobotanical records from Europe and the northern Tethyan region are not yet reliably correlated with any climatic event. The Eocene Krappfeld sequence, with abundant and diverse palynoflora, is a continental sedimentary sequence that can be positively correlated with the EECO, and therefore represents an opportunity to develop continental climate records to complement those from marine settings.

This paper presents a multidisciplinary study combining palynology with LM and SEM, lipid biomarker analysis and clay mineralogy of sedimentary rocks from the EECO of the Eastern Alps. This is the first high quality terrestrial palynological record from the northwestern Tethyan region. Here we discuss the changes in depositional environment that contextualize our analyses, the dominant vegetation through the study interval with implications for the overall ecology of the Tethyan EECO, and interpretation of continental climate derived from vegetation and biomarker assemblages.

2. Geographical and geological setting

The Krappfeld area is situated in the state of Carinthia in southern Austria. The section investigated (coordinates: 46° 50´ 27" N, 014° 31´ 35" E) was exposed in the Pemberg Quarry west of Klein St. Paul (Fig. 1), but unfortunately, this classical outcrop was filled for recultivation and is no longer accessible. The exposed rocks represent the upper part of the Gosau Group, which in the Eastern Alps comprises mainly siliciclastic and mixed siliciclastic-carbonate strata deposited on sedimentary and metamorphic units after Early Cretaceous thrusting. Deposition of the Gosau Group was the result of transtension, followed by rapid subsidence into deep-water environments due to subduction and tectonic erosion at the front of the Austro-Alpine microplate (Wagreich 1993, 2001). Facies patterns in the Paleogene were controlled by the SW-NE trending Penninic basin, which separated the European and Adriatic lithospheric plates. The Gosau deposits accumulated at the southern margin of this basin on the north-facing continental slope and the shelf of the Adriatic Plate.

The Gosau Group in the Krappfeld area comprise the Campanian to Middle Eocene (von Hillebrandt, 1993; Wilkens, 1989). The Paleogene rests with an erosional unconformity on the Campanian. This stratigraphic gap was interpreted as the result of a major sea-level drop in the latest Paleocene (Egger et al., 2009). At the base of the Paleogene succession, terrestrial red claystone with intercalations of coal seams (Holzer Formation) occur. Previously published surveys reveal highly diverse and well preserved palynofloras, but these originated from individual samples without information regarding their exact location in the succession, and the biostratigraphic and sedimentological context was not clear (Hofmann and Zetter, 2001; Zetter and Hofmann, 2001). A major transgression in the Ypresian (early Biochron NP12 – Egger et al., 2009) flooded the shelf and brought back marine conditions.

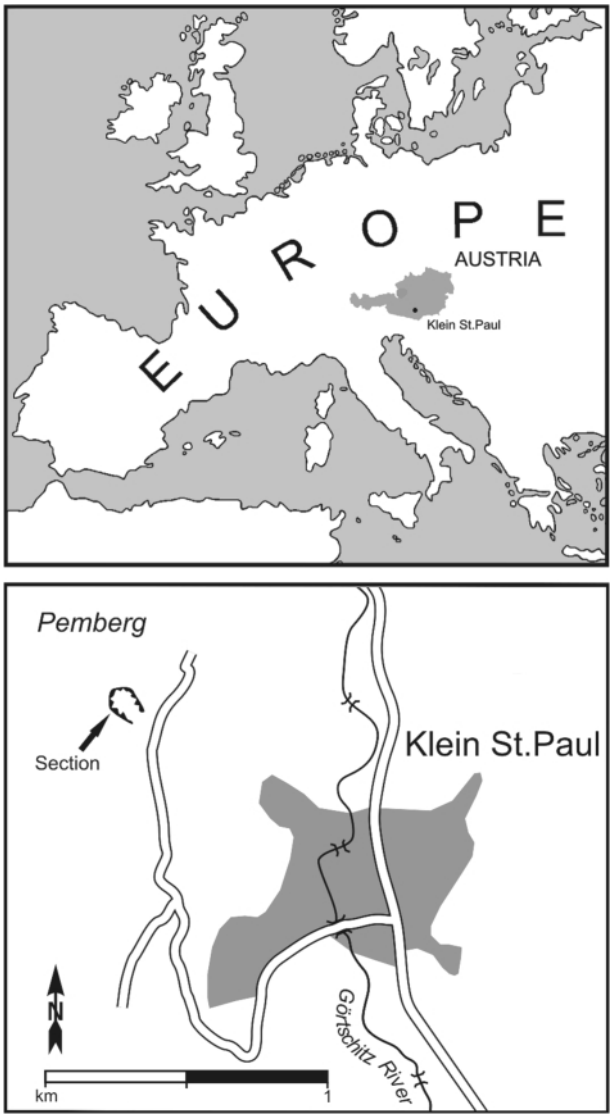

Figure 1: Sketch map of the locality Pemberger Quarry.

3. Methods

3.1 Palynology

Terrestrial palynomorphs were recovered by standard procedures: Samples were crushed by hand with a mortar and pestle, and the powder dissolved with standard wet chemical processes using HCl and HF. The organic residue was not sieved to retain palynomorphs smaller than 10µ, and then acetolyzed, mixed with glycerine and stored in small glass bottles. For LM examination, a drop of well-mixed organic residue and glycerine was evenly distributed on a glass slide. Each sample was screened carefully, using up two to nine slides to yield both common and, most importantly, the accessorial taxa. The latter do occur generally in very small numbers. The extremely low counts (below five, e.g., fernspores) in the nearly barren samples (PQ 6, PQ7 and PQ10) despite screening two or three slides per sample have been neglected. For LM photography (Samsung digital camera on a Nikon microscope) the pollen grains were transferred by a hair on a preparation needle in a clean drop of glycerine on a new slide. For examination under the SEM (FEI Inspect 500), the same pollen grains were removed with a micromanipulator to a SEM stub, rinsed with 100% alcohol to remove the glycerine and sputtered-coated with gold. Stubs are stored in the Department of Palaeontology, University of Vienna.

2.2 Nannoplankton

For calcareous nannoplankton stratigraphy in the Campanian, smear-slides of four samples were studied with a light

microscope under parallel and crossed polarisation filters at a magnification of 1000x. Species richness is medium in the studied samples (18 taxa on average) and the majority of the specimens are slightly etched but all taxa were easily identified. Here only the species crucial for the age assignment of the samples in the calcareous nannoplankton zonation (CC zones) of Sissingh (1977) are mentioned. The reader is referred to Burnett (1998) for nannoplankton taxonomy.

3.3 Biomarker analyses

Lipid biomarker extraction and fractionation. For biomarker analyses, the powdered samples were extracted via Soxhlet apparatus for 24 h using dichloromethane (DCM)/MeOH (2:1 v/v) as the organic solvent. The total lipid extracts were separated into two fractions using a column packed with (activated) alumina by elution with hexane (saturated hydrocarbon or apolar fraction) and DCM/MeOH (1:2 v/v; polar fraction). Individual compounds were identified and quantified relative to internal standards (5α-androstane, apolar fraction; hexadecan-2-ol, polar fraction) using gas chromatography (GC) and gas chromatography-mass spectrometry (GC-MS). Prior to analysis, polar fractions were silylated with BSTFA (N,O-bis(trimethylsilyl)trifluoroacetamide). GC analysis was performed on a CarloErba Gas Chromatograph equipped with a flame ionisation detector (FID) and fitted with a Chrompack fused silica capillary column (50 m x 0.32 mm i.d.) coated with a CP Sil-5CB stationary phase (dimethylpolysiloxane equivalent, 0.12 µm film thickness). GC-MS analysis was performed on a Thermoquest Finnigan Trace GC interfaced with a Thermoquest Finnigan Trace MS operating with an electron ionisation source at 70 eV and scanning over m/z ranges of 50 to 850 Daltons. The GC was fitted with a fused silica capillary column (50 m x 0.32 mm i.d.) coated with a ZB1 stationary phase (dimethylpolysiloxane equivalent, 0.12 µm film thickness). For both GC and GC-MS, 1µl of sample was injected at 50°C using an on-column injector. The temperature was increased to 130°C with an initial ramp of 20°C/min, then to 300°C at 4°C/min, followed by an isothermal for 20 min.

High performance liquid chromatography/atmospheric pressure chemical ionisation – mass spectrometry (HPLC/APCI-MS) was used for the analysis of GDGTs. Analysis was conducted on filtered neutral polar fractions using a Thermo Scientific TSQ Quantum Access equipped with Accela Autosampler, Accela Pump and Xcalibur software. Separation was achieved with an Alltech Prevail Cyano column (150 mm x 2.1 mm; 3 µm stationary phase thickness), and injection volumes varied from 10 to 20 µl in partial loop-no waste injection setting, or 25 µl in full loop injection setting. GDGTs were eluted isocratically with 99% A and 1% B v/v for 7 min, then a linear gradient to 1.6% v/v B in 43 min, where A = hexane and B = iso-propanol. Flow rate was 0.2 ml/min. Detection was achieved using atmospheric pressure positive ion chemical ionization mass spectrometry (APCI-MS) analysis of the eluent; conditions were: corona discharge current 4 µA, vapouriser temperature 355°C, capillary temperature 280°C and sheath gas 0.15 L/min. Ion detection was performed in selective ion monitoring (SIM) mode. The m/z values selected relate to the $[M+H]^+$ (protonated molecular ion) of the isoprenoidal and branched GDGT analytes (Schouten et al., 2007).

3.4 Clay minerology

For mineralogical analyses the samples were studied by means of X-ray diffraction (XRD) using a Panalytical X´Pert Pro MPD diffractometer with automatic divergent slit, Cu LFF tube 45 kV, 40 mA, with an X´Celerator detector. The measuring time was 25s, with a stepsize of 0,017°. Bulk samples as well as the clay fractions (<2µm) were analysed.

Sample preparation generally followed the methods described by Whittig (1965) and Tributh (1989). Dispersion of clay particles and destruction of organic matter was achieved by treatment with dilute hydrogen peroxide. Separation of clay fraction was carried out by using centrifugation methods. The exchange complex of each sample (<2µm) was saturated with Mg and K using chloride solutions by shaking. Similar to the methods of Kinter and Diamond (1956) the preferential orientation of the clay minerals was obtained by suction through a porous ceramic plate. To avoid disturbance of the orientation during trying, the samples were equilibrated during 7 days above saturated NH_4NO_3 solution. Afterwards expansion tests were made, using ethylenglycol, glycerol and DMSO as well contraction tests heating the samples up to 550 C. After each step the samples were X-rayed from 2-40 °2θ.

The clay minerals were identified according to Thorez (1975), Brindley and Brown (1980), Moore and Reynolds (1997) and Wilson (1987). Semiquantitative estimations were carried out using the corrected intensities of characteristic X-ray peaks (Riedmüller 1978). Semiquantitative mineral composition of the bulk samples was estimated using the method described by Schultz (1964).

3.4.1 Simultaneous Thermal Analysis (STA)

Thermal analysis in clay mineralogy provides additional information about the clay minerals in a sample and is therefore used more and more in clay science. Clay minerals contain different amounts of hydroxyl groups which are liberated when energy is absorbed. Clay minerals also undergo considerable weight losses at moderate temperatures. Under 1000 °C many lattice transformations in the clay minerals take place which are also reflected as energy changes (Mackenzie, 1964). Thermogravimetric (TG) and Differential Scanning Calorimetry (DSC) measurements were done. The STA analyses were carried out on Netzsch STA 409 PC Luxx®. Between 50 and 51 mg of the sample were weighed in a Pt-cup and then analysed in a controlled atmosphere with 50 ml/min air and 10 ml/min N_2. The heating rate was 10° K/min, the samples were heated up to 1000°C.

4. Description and biostratigraphy of the section

The lower part of the sedimentary succession is formed by

5-m thick silty grey marlstone of the upper Pemberger Formation. The marlstone is rich in calcareous nannoplankton. At the base (sample PQ1) of the succession, *Uniplanarius trifidus* co-occurs with *Broinsonia parca*, *Eiffellithus eximius*, and *Reinhardtites levis*. These species are indicative for the upper part of the *Uniplanarius trifidus* Zone (CC 22b). *U. trifidus* is very

Family (subfamily)	taxon/ botanical affinity	number				temp./	meso./	megath.	sea-	Zonobio.	extant
		of taxa	PQ5	PQ8	PQ9	mesoth.	megath.		sonality	Zonoeco.	distribution
Filicophyta	fern taxa	12	65%	3.4%	13%	x	x	x	?	II - VII	cosmopol.
?Annonaceae	indet.	1		0.2%			x		?	I - VI	America, Africa, Asia
Alangiaceae	*Alangium villosum*-type	1		0.1%				x	no	I	NE-Australia, Java, Phillip.
Anacardiaceae	*Lannea*-type	1	1%	2%	1%			x	no	I (- II)	Africa, Indomal.
	?Spondias-like	1		2.5%				x	no	I (- II)	SE Asia-Indomal
	indet.	1	3.5%	3%			x		?		?
Aquifoliaceae	*Ilex*	2	3%	2%	1.5%	x	x		yes	II-VII	cosmopol.
Araceae	indet.	1							?	?	?
Monsterae	*Proxapertites operculatus*	1	1%	2%	1.5%		x		?	I	pantropisch
Arecaceae											
Arecoideae	*Aiphanes*-type	1		0.5%				x	yes	I/II, II/I	Central - NW S. America
	Dypsis-like	1			2%			x	yes	I - II	Madagascar
	Elaeis-like	2	19.7%					x	no	I/II - II/I	S. Amer, Africa
Calamoideae	*Calamus*	4	1%	3.5%	2.5%			x	no	I/II - II/I	Old world tropics
	Salacca-type	1		1%				x	no	I - II	Indomal.
Ceroxyloideae	*Ravenea*-type	1		0.5%				x	yes	I - II	Madagas., Comoro I.
Coryphoideae	*?Brahea*-like	1		0.5%	1%		x	x	yes	I - II	Central America
Nypoideae	*Nypa*-type	1		6%				x	no	I	India to Solomon I.
indet.		5	13.8%	6%	4.5%		x	x	?	I - IV	?
Avicenniaceae	*Avicennia*-type	1		0.5%			x	x	yes	I, II - II/V	pantropical
Betulaceae	*Alnus*	1		0.5%	0.2%	x			yes	II - XIII	north. Hemisphere
Bignoniaceae	*?Pithecoctenium*-like	1		0.1%			x		no	I - II	trop. America
Burseraceae	*Canarium*-type	1	0.5%	0.5%	0.1%			x	no	I - II	Indomal.
Calycanthaceae	*?Chimonanthus*-like	1		0.2%		x			yes	IV - VII	China
Chloranthaceae	*?Ascarina*-like	1	0.2%	0.2%			x		yes	II - VI	Madagas.-New Zeal.
Euphorbiaceae	*Leucroton*-type	1		0.5%			x	x	yes	II/I - II	Caribean
	Sebastiana-like	1		0.5%	0.1%		x	x	yes	I - II	pantrop.
	Stillingia-like	1		1.2%	0.1%		x	x	yes	I - II	Amer., Madag., Malay.
Fabaceae											
?Caesalpinoideae	indet	1	0.5	0.5%					?		?
Fagaceae	*Lithocarpus*	2	3%	14.2%	5%		x		yes	I - II	Indomalesia
	Eotrigonobalanus	1	1%	4%	4%				?		extinct
Hamamelidaceae	*Corylopsis*-like	1		0.5%		x			yes	V -VI?	Bhutan-Japan
Icacinaceae	*Iodes*-type	1		0.5%				x	no	I - II	Old world tropics
Juglandaceae	extinct *Normapolles* s.l.	>8	8.9%	42%	19%				yes		extinct
	Engelhardia-type	2	5.5%	3.4%	6.5%	x			yes	V - VI	Himalya-Malesia
	Platycarya-type	2	7%	3.6%	7.5%	x			yes	V - VI	China-Japan
Liliaceae	indet	1			0.2%				?		?
Malvaceae											
Bombacoideae	*Rhodognaphalopsis*-type	1		0.5%				x	no	I - I/II	trop. America
Helicteroideae	*Durio*-type	1		0.2%				x	no	I/II, II /I - II	Myanmar - W Males.
Sterculiodeae	indet	1	0.5%	0.5%			x		?		?
Tilioideae	*Craigia*	1	0.5%	2.5%	0.2%		x		yes	V	SW China
Myricaceae	indet.	4	3%	10%	12.5%		x		yes	II - VI	?
	Myrica	1	6%	14%	7%	x			yes	V -VII	subcosmopolitan
Nyssaceae	*Nyssa*	1	1%	2%	0.2%	x			yes	V	America, China
Olacaceae	*Anacolosa*-type	1		0.5%				x	yes	I - II	Madagas., Afr.
Oleaceae	indet.	1		0.5%					?		?
Picrodendraceae	*Aristogeitonia*-type	1	1%	4.5%	0.2%			x	yes	I/II - II/I	Africa, S America
Platanaceae	*Platanus*	1			0.2%	x			yes	V-VII	northern hemisphere
Restionaceae	*Restioniidites*-type	1	0.5%	1.5%			x		yes		south. hemisphere
Rhizophoraceae	*Ceriops*-type	1		0.5%				x	no	I, II - II/V	Indian & Pacific oceans
Rhoipteleaceae	*Plicapollis*	1	2%	9.6%	6.5%	x			yes	V - VI	SW China, N Vietnam
Rutaceae	indet.	1	1%	2.5%	0.1%		x		yes		?
	Zanthoxylon-type	1	0.5%	0.5%	0.1%		x		yes	I - II	Am., Africa & Asia
Sapotaceae	*Palaquium*-type	1		1.5%	0.2%		x		yes	I, II/I, - II	Taiwan - Indomalesia
	Pouteria-like	1	2%	2%			x		yes	I - II	pantropical
	?Tieghemella-like	1	1%	2.5%				x	no	I, I/ II	W Africa
Simaroubaceae	indet.	1	1%	1.5%	2.7%		x		yes		Americas, Asia
Styracaceae	*Styrax japonica*-type	1		0.5%			x		yes	II - VI	pantropical
	indet.	1		0.5%	0.1%		x		yes		?
Theaceae	*Camellia*-like	2		0.5%			x		yes	II - V	E Asia - Indomalesia
Thymelaceae	*Wikstroemia*-type	1		0.2%			x		yes	I - II	SE Asia - Pacific
Vitaceae	*Vitis*	1	0.5%			x			yes	V - VII	north. hemisphere
fam. Indet	gen. Indet		3.5%	4.5%	2%						
	slides counted		9	7	6						
	sum of counts		2600	3560	2800						

Table 1: Summary of all angiosperm pollen taxa encountered so far from the Holzer Formation, their botanical affinity, their approximated climatic requirements and today distribution of extant relatives (information from Dransfield et al., 2008, Gentry, 1996, Mabberly, 2000) and their approximated zonobiomes, zonoecotones (after Walter and Breckle, 1999).Temp.-mesoth. = temperate to mesothermal, meso.-megath. = mesothermal to megathermal, seasonality = profound changes in precipitation and temperature during the year.

rare in this sample and does not occur in the other samples. Nonetheless, the other three mentioned species indicate the same age assignment for samples PQ2 and PQ3. In the highest sample (PQ4), *E. eximius* does not occur anymore. Therefore, this sample is attributed to the lower part of the *Tranolithus phacelosus* Zone (CC23a). According to Gradstein et al. (2004), sub-Zones CC22b and CC23a are of early Late Campanian age. This age assignment of the Pemberger Formation at its type-locality is consistent with previous studies on ammonites (Thiedig and Wiedmann, 1976) reporting on the stratigraphically important species *Pseudokossmaticeras tercense* and *P. brandti*. Both species are indicative for the *Nostoceras hyatti* Zone of Late Campanian age (Küchler and Odin, 2001). *Pachydiscus haldemsis* and a dinoflagellate assemblage (e.g. *Apectodinium deflandrei*, *Cannosphaeropsis utinensis*, *Dinogymnium acuminatum*, *Glaphyrocysta expansa*, *Hystrichosphaeridium tubiferum*, *Palaeohystrichophora infusorioides*, *Pervosphaeridium intervelum*, *Xenascus ceratioides*) support this age assignment (Soliman et al., 2009).

The Pemberger Formation is unconformably overlain by 8 m-thick soft clay of the Holzer Formation, which is devoid of carbonate. The green and red clays (PQ6 and PQ7) do not contain any marine fossils but the lenses of coaly clay at the base of the Holzer Formation are rich in terrestrial palynomorphs (sample PQ5). A different palynoflora (sample PQ 8), characterized by the co-occurrence of numerous marine dinoflagellates, occurs in the black transgressive shales. The shale is overlain by less than a half meter thick yellow, weathered sand with ca. 50 cm of gray clay with dark gray bands (sample PQ9) on top. The Holzer Formation is then overlain by the nummulitic limestone and marlstone (samples PQ 10, 10a, and 11) of the Sittenberg Formation (Thiedig et al., 1999). In the Pemberger quarry, *Assilina placentula*, *Nummulites burdigalensis kuepperi*, *Nummulites increscens*, and *Nummulites bearnensis* have been described from the base of this marine unit (Schaub, 1981; Hillebrandt, 1993). This faunal assemblage is indicative of the lower part of shallow benthic zone SBZ10, which has been correlated with calcareous nannoplankton zone NP12 (Serra-Kiel et al. 1998).

5. Results

5.1 Palynology

Three lithologies rich in palynomorphs were identified, with representative examples illustrated in Plate 1 A-O and Plate 2 A-O. All pollen data, in percent, are given in Table 1 (as well as modern climatic requirements and distributions). Sample PQ5, positioned at the base of the Holzer Formation, is characterized by abundant and diverse fern spores (Schizaeales: *Cicatricosporites* spp., *Ischyosporites* sp. *Leiotriletes* spp. and various Polypodiaceae s.l.), lumps of fern spores, and various monosulcate Arecaceae (*Monocolpopollenites* spp. affiliated to extant *Elais* sp.; Plate 1 G-I; *Arecipites* spp.), Myricaceae and Juglandaceae (*Platycarya*). Samples PQ6 and PQ7, from the red and green clays respectively, are nearly barren of any palynomorphs and microscopic organic matter (see Corg data below) and contain only few poorly preserved fernspores (Schizaeales and Polypodiaceae s.l.). The palynomorph assemblage of sample PQ8 from the black transgressive shale is characterized by the co-occurrence of marine dinoflagellates and terrestrial palynomorphs. More than 90% of the dinoflagellate assemblage are specimens of the peridinoid genus *Apectodinium* (*A. homomorphum*, *A. parvum*, *A paniculatum*, and *A. spp*). In addition, *Homotryblium pallidum* and *Spinidinium echinoideum* also occur (Mohamed in Drobne et al., 2011). With respect to the terrestrial palynomorphs, these sediments contain particularly abundant *Normapolles* s.l., *Nypa* (Plate 1 A-C) and various calamoid palm pollen (Plate 1 D-F), and the presence of *Avicennia* (Plate 2 D-F) and *Ceriops* should be mentioned. Sample PQ9 from the grey and dark grey clays is dominated by triporate taxa such as *Normapolles* s.l., Myricaceae, Juglandaceae and Rhoipteleaceae, but calamoid and monosulcate palm taxa and numerous fern spores are also present. Sample PQ10 is devoid of terrestrial palynomorphs, but contains abundant *Apectodinium* spp.

In general, the facies-dependant terrestrial pollen and spore assemblages are quite diverse. To date, ca. 84 angiosperm taxa and ca. 12 fern taxa have been identified, but investigation is still ongoing. The routinely applied combination of LM and SEM is essential to affiliate the pollen taxa at least down to genus level. These results are important for further climatic and ecological qualitative interpretations because the ecological and climatic amplitudes of a family can vary consistently (e.g., in the Fagaceae, Euphorbiaceae, Caesalpinoideae, Hamamelidaceae, Rutaceae, Anacardiaceae, Oleaceae and many more).

The identifiable angiosperm pollen grains are dominated quantitatively (more than 80% of the individual pollen) by generally wind-pollinated temperate to mesothermal families (comprising ca. 18% the genera and species list, e.g., Fagaceae: *Lithocarpus*, *Trigonobalanopsis*, Juglandaceae: extinct *Normapolles* s.l., *Platycarya*-types, *Engelhardia*-types, Myricaceae: extinct, *Myrica*-types, Rhoipteleaceae: *Plicapollis*-type), and to a lesser extent Aquifoliaceae (*Ilex*-types). The remaining approximately 20% of the pollen sum (all grains counted) come from the insect pollinated mesothermal/megathermal and true megathermal families. The mesothermal/megathermal taxa comprise ca. 45% of the floral list (e,g, Avicenniaceae: *Avicennia*-type, black mangrove, Calycanthaceae, Chloranthaceae, Euphorbiaceae: *Leucroton*-type, Plate 2 M – O; Hamamelidaceae: *Corylopsis*-like, Plate 2 G- H, Picrodendraceae *Aristogeitonia*-type, Styracaceae: *Styrax japonica*-type and indet., Theaceae: *Camellia*-like, and Thymelaeaceae: *Wikstroemia*-type, Plate 2 A -C) and true megathermal families comprise ca. 34 % of the floral list (e.g., Alangiaceae: *Alangium villosum*-type, Plate 1 J – L, Anacardiaceae: *Lannea*-type and Spondias type, most of the Arecaceae with at least 16 palm taxa (e.g., Arecoideae, Calamoideae, Ceroxyloideae, Coryphoideae and Nypoideae subfamilies, Bignoniaceae: *Pithecoctenium* like, Burseraceae: *Canarium*-type, Icacinaceae:

Iodes-like, Malvaceae: Helicteroideae-*Durio*-type, Bombacoideae-*Rhodognaphalopsis*-type, syn. *Pachira*, Olacaceae: *Anacolosa*-type, Plate 1 M - O, Rhizophoraceae: *Ceriops*-type, Sapotaceae: *Palaquium* and *Pouteria*). The rest (ca.3 %) of the taxa are not assignable to any particular climatic conditions.

5.2 Organic carbon and lipid biomarker characterisation

The base of the section (sample PQ5), is characterized by a green clay with small lenses enriched in coal matter. These lenses contain 2.2 wt% of organic carbon (C_{org}), whereas the pure green clay displays much lower C_{org}-values of 0.1 wt%. The main part of the clay (sample PQ7) is red colored and has a C_{org}-content of 0.2 wt%. With a sharp stratigraphic contact the red clay is overlain by 0.5 m thick black clay (sample PQ8) containing 7.6 wt% C_{org}.

Lipid biomarker analyses were conducted on PQ5, PQ8 and PQ9 as part of an initial survey of organic matter sources and to test the feasibility of further investigations. All samples are characterized by the excellent preservation of diverse apolar (primarily n-alkanes and hopanes) as well as polar lipids (fatty acids, triterpenoids). The n-alkanes range in carbon number primarily from C_{19} to C_{32}, with a pronounced odd-over-even predominance especially among the higher molecular weight homologues that is indicative of an origin from higher plant leaf waxes (e.g.Eglinton et al., 1962; Eglinton and Hamilton, 1967; Kolattukudy, 1976). Similarly, the n-alkanoic acids range in carbon number from C_{16} to C_{30}, with an even-over-odd predominance, consistent with a leaf wax origin for the higher molecular weight components (>C_{24}). A variety of triterpenoid acids and the abundant hopanoids provide further evidence for a predominantly terrestrial source for the organic matter in all three horizons.

The presence of functionalized compounds, such as sterols and fatty acids, provides direct evidence for the relatively low thermal maturity of these sediments. Further evidence comes from the persistence of an odd-over-even predominance of the n-alkanes. The hopanes, especially the C_{27}, C_{29}, C_{30} and C_{32} components, are dominated by those isomers with the biological 17β,21β(H) configuration (ca 70 to 90%, depending on sample and specific hopane). 17β,21α(H) isomers also present and the thermally stable 17α,21β(H) isomers are absent, again consistent with a low thermal maturity for this section (e.g. Peters and Moldowan, 1991; Peters et al., 2005). The exception to these observations are the C_{31} (homohopane) components, which are dominated by the 17α,21β(H) isomer; we suggest that this derives from decarboxylation of 17α,21β(H)-bishomohopanoic acid which can arise from acid catalysed conversion in, for example, peat-forming environments (e.g. Pancost et al., 2003, references therein).

PQ5, positioned at the base of the Holzer Formation, is characterized by abundant odd-carbon-number n-alkanes with a unimodal distribution, dominated by the C_{27} and to a lesser degree the C_{29} homologues. The aforementioned hopanes are also abundant, in fact occurring at concentrations similar to those of many of the n-alkanes. The polar fraction contains low concentrations of C_{16}, C_{18}, C_{20} and C_{22} n-alkanoic acids, higher concentrations of the C_{24} and C_{26} homologues and highest concentrations of the C_{28} and C_{30} acids. Also present are hopanoic acids and various triterpenoid acids. PQ8, representing the black transgressive shale, is characterized by an almost identical suite of biomarkers, including n-alkanes dominated by the C_{27} homologue and n-alkanoic acids dominated by the C_{28} and C_{30} homologues. This suggests that despite the different lithology, the black shale organic matter assemblage was still dominated by terrigenous inputs.

Sample PQ9 from the grey and dark grey clays is also characterized by abundant n-alkanes and n-alkanoic acids, but the distributions of those compounds are somewhat different than in PQ5 and PQ8. The n-alkanes are still dominated by the C_{27} homologue, but lower molecular weight components (C18-C26, including both odd and even-carbon num-

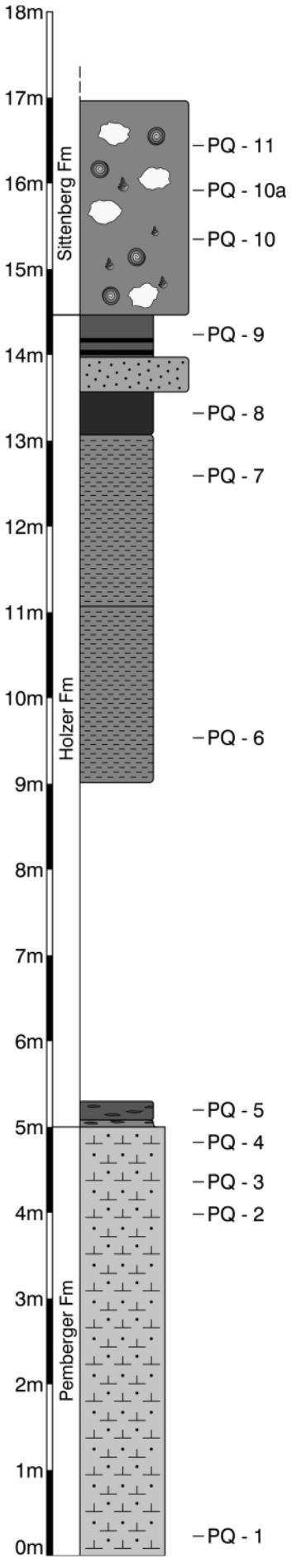

Figure 2: Profile of the lithology of the topmost Pemberger Formation, the Holzer Formation and the lowermost Sittenberg Formation in the Pemberger quarry with indicated sample horizons.

bered compounds) are relatively more abundant than in PQ5 and PQ8. Hopanes are very abundant especially relative to other compounds in the apolar fraction, and in fact the 17α,21β (H)-homohopane occurs at the same concentration at the most abundant n-alkane. The n-alkanoic acids comprise a range from C_{16} to C_{30} as observed in the other sediments, but the even-over-odd predominance is markedly reduced, the low-molecular-weight C_{16} and C_{18} homologues are relatively more abundant (although still subordinate to the HMW components), and most strikingly the HMW distribution is dominated by the C_{24} and C_{26}, rather than the C_{28} and C_{30} homologues.

LC-MS analyses of glycerol dialkyl glycerol tetraether (GDGT) distributions confirm these interpretations. Signals were weak, even in selected ion monitoring mode, but the dominant GDGTs could be identified in PQ5 and PQ9. In both, the predominantly marine archaea derived crenarchaeol is present in only trace concentrations, and soil bacteria derived branched and cyclic GDGTs are markedly more abundant; calculation of Branched Isoprenoid Tetraether (BIT) indices is limited due to the low concentrations but values are between 0.9 and 1.0, well within the range of organic matter dominated by terrigenous inputs (Hopmans et al., 2004). Methyl branching and cyclisation indices (MBT/CBT) for the branched GDGTs could be determined and these can be converted to soil pH and mean annual air temperatures (MAT; Weijers et al., 2007) but the analytical error is very large due to low peak areas (for pH: ± 0.1 unit, in addition to the ±0.3 pH units associated with the calibration; and for temperature: ±3ºC, in addition to the ±5ºC error associated with the calibration). The estimated pH estimates are 6.8 and 6.5 for PQ5 and PQ9, respectively, and the estimated MAT is 17ºC for PQ5, although these should be treated with caution.

5.3 Clay mineralogy

Mineralogical analyses of samples PQ4 to PQ10 yielded abundant kaolinite. In three of the six analysed samples the amount of kaolinite ranges from 73 to 78% by mass, whilst in the remaining samples have 47- 64% kaolinite by mass and PQ10 has 25% by mass. Well crystallized kaolinite and poorly crystallized so-called fire clay occur in approximately equal parts. Illite is the second most abundant clay mineral in the profile, representing 17 to 47% by mass. Smectite is present in all samples but never represents more than 28% of the mass and is typically much lower. Chlorites were not detected in any of the analysed samples. The bulk samples contain layer silicates, representing up to 82% by mass, and smaller amounts of quartz in the range from 14 to 36% by mass. Only two samples, PQ4 and PQ10, contain calcite (40% and 10%, respectively). Hematite is also present in PQ7, the sample containing the highest amount of kaolinite.

The grain size distribution of the kaolinite-rich samples is dominated by the clay fraction <2µm, which is up to 67%. PQ4 contains the highest amount (59%) of silt, and only PQ10 has high amounts of sand (32%) and silt (51%).

6. Discussion

6.1 Stratigraphy

Egger et al. (2009) attributed the marine transgression in the Krappfeld Eocene to a eustatic event in the late calcareous nannoplankton Biochron NP11 or in early Biochron NP12 (ca. between 53 and 52 Ma) within Chron 24n. In the tectonically influenced Belgian basin four transgressive events are present, with the sea-level rise during the uppermost NP11 and NP12 Biochrons (53 to 50.5 Ma; Vandenberghe et al., 2004) occurring during the EECO. At Krappfeld, the base of the transgressive succession is formed by a black shale (sample PQ8) containing abundant dinoflagellates dominated by *Apectodinium* ssp. but also abundant terrestrial pollen. The calcareous NP12 zone of the overlying lowermost Sittenberg Formation corresponds either to the onset of the EECO after Zachos et al. (2001), or the lower part of the EECO (Muttoni and Kent, 2007) and also spans the middle of the EECO in the Belgian Basin (Vanhove et al., 2011 and references therein). The directly underlying terrestrial influenced Holzer Formation is interpreted to represent at least the lower part of the NP12 zone and is therefore assigned to the warmest extended period of the Cenozoic. This is also corroborated by the composition of the palynoflora and the lack of typical Paleogene pollen markers. The mega- to mesothermal families and genera had enough time to either migrate to the Krappfeld area and/or to diversify into several species, establishing a

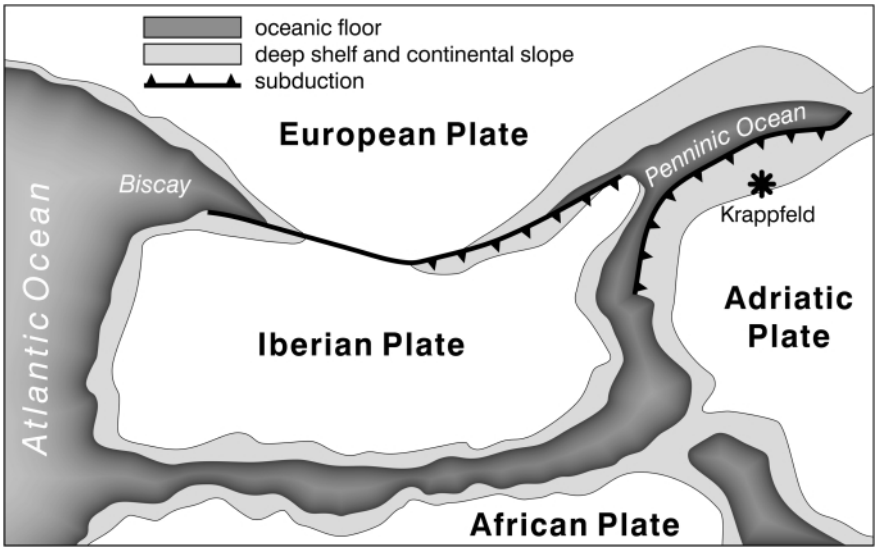

Figure 3: Schematic paleogeographic map showing the position of the Alpine environmental areas in the early Paleogene (simplified and modified after Stampfli et al., 1998).

new vegetation regime. This regime was particularly diverse in palm species, comprising up to seventeen Arecaceae taxa, and several megathermal Anacardiaceae, Sapotaceae and Malvaceae taxa, which can be interpreted to represent a Tethyan equivalent of the London Clay diaspore floras (compare Collinson, 1983).

6.2 Facies

The lithologies and palynomorph assemblages of the studied section represent three different facies from bottom to top: (1) coal-bearing palm swamp, (2) coastal near swamp with mangroves, and (3) shrubby back swamp; overall, these transitions reflect the migration of the coastline in this section.

The coal-bearing palm swamp facies (sample PQ5) contains abundant fern spores (Schizaeales and Polypodiaceae) often occurring in lumps, palm pollen (*Monocolpollenites* spp. = presumable modern equivalent *Elais*; for *M. cf. tranquilus* and *Arecipites* spp. modern equivalents have not been found) occasionally preserved in lumps, *Emmapollis* (Chloranthaceae), *Proxapertites operculatus* (Araceae), Sapotaceae (*Palaquium*-type) and Myricaceae. This indicates a boggy palm swamp facies with herbaceous (ferns and Araceae) and shrubby undergrowth (Myricaceae), and this interpretation is consistent with the dominance of higher plant and bacterial biomarkers and the relative dearth of algal biomarkers (e.g. sterols or steranes). Myricaceae undergrowth is known from the Cenozoic onwards (Hofmann et al., 2002; Hofmann and Zetter, 2005, Ewel, 1992), and coastal near boggy palm swamps with fern undergrowth occur in contemporary tropics (Hofmann, 2002).

The coastal near swamp facies (sample PQ8) is distinguished from the other facies by the presence of abundant dinoflagellates. The palynoflora comprises the dominant triporate taxa, but also several calamoid palm taxa, unknown palm taxa, *Nyssa*, megathermal Anacardiaceae, Sapotaceae, Malvaceae with mangrove elements such as *Nypa*, *Avicennia*- and *Cerio-ops*-type pollen. Despite the coastal and clearly marine-influenced setting, the pollen assemblages and biomarker distributions (the latter dominated by terrigenous biomarkers similar to those of PQ5) indicate that the organic matter was still terrigenous. The terrestrial pollen and biomarkers suggest that the site was still proximal, and we suggest that the shale deposition was related to both eustatic sea level rise and irregular bottom topography, where organic rich material accumulated (been washed or slumped) into topographic hollows (see review in Wignall, 1994).

The shrubby back swamp facies (sample PQ9) comprises mostly triporate taxa (e.g., Myricaceae, *Normapolles* s.l., Juglandaceae), ferns and few calamoid and very small monsulcate palm pollen taxa (probable affiable to *Brahea* and *Dypsis*, see Dransfield et al., 2008) and Araceae (*Proxapertites operculatus*). Shrubby back swamp settings with vegetation dominated by Myricaceae have been recorded from the Eocene (Hofmann and Zetter, 2001, Zetter and Hofmann, 2001), the Miocene (Hofmann and Zetter, 2005, Hofmann et al., 2002) and today (Ewel, 1992). Although biomarker assemblages of PQ9 are still dominated by terrigenous inputs, the different n-alkane and n-alkanoic acid distributions are consistent with a different dominant plant input. The much higher abundance of hopanoids relative to n-alkyl compounds also suggests different depositional conditions than those associated with the other facies.

6.3 Palaeoclimate interpretation

The palynoflora in all three facies are dominated qualitatively by angiosperms (87 %, 84 of 96 of the pollen and spore taxa); of these, ca 85% are woody plants and the rest are herbaceous and fern plants. This high percentage of woody taxa is characteristic for tropical and subtropical floras (Mabberly, 1992; Vareschi, 1980; Whitmore, 1992). However, in the Krappfeld, wind pollinated plant pollen dominates quantitatively (pollen counts: PQ5 35% beside 60% fernspores, PQ8 over 80% beside 3,4% fernspores, PQ9 53% beside 13% fernspores). Generally, wind pollinated families produce far more pollen than entomophilic (insect pollinated) plants and, therefore, pollen of these taxa are more abundantly preserved in sedimentary rocks (Faegri and Iverson, 1989; Klaus, 1987).

Taxa with temperate/mesothermal requirements are quantitatively over-represented in the pollen sum, despite these pollen grains originating from only 18% of the taxa of the floral list. This has also been observed in the previously investigated Krappfeld samples (Hofmann and Zetter, 2001; Zetter and Hofmann, 2001) and is also true for most of the Miocene localities of Austria (Hofmann and Zetter, 2005, Hofmann et al., 2002).

Pollen from insect pollinated plants are preserved in low numbers (accessorial pollen in the pollen sum), such that pollen of these taxa are generally under-represented in the geological record (Reddi and Reddi, 1986 and summarized in Hofmann, 2002). In the Krappfeld they are generally coming from taxa for which modern equivalents prefer mesothermal/megathermal and true megathermal climatic conditions (Hofmann and Zetter, 2001, Zetter and Hofmann, 2001). However, these accessorial taxa qualitatively dominate (approximately 80%) the spectra of the entire pollen list.

Mesothermal/megathermal taxa and some of the true megathermal taxa (ca. 52 % of all taxa; see table 1) occur today in seasonally controlled (passat-like or monsoon-like precipitation) climatic conditions. Specifically, they exist today in the zonobiome II (= subtropical humid to arid summer rain climate with deciduous woody plants and grasslands; definition after Walter and Breckle, 1999). Only approximately 22% of the identified angiosperm taxa have modern equivalents growing in tropical everwet conditions of zonobiome I (= tropical, equatorial humid day time climate with evergreen rainforests, with eventually one to two drier months with only 250 mm rain; definition after Walter and Breckle, 1999). Seasonality cannot be readily inferred from about 26% of the taxa. Together with the assumed more temperate taxa, this composition of mesothermal to megathermal, everwet and seasonal controlled floral elements suggests a biome at or spanning the transition be-

tween zonobiome II and zonobiome I, which today is expressed by the zonoecotone I/II (= seasonally controlled mosaic of deciduous and evergreen forests that are also influenced by relief, complex hydric and edaphic conditions, Breckle and Walter, 1999). The estimated pH estimates of 6.8 and 6.5 for PQ5 and PQ9, respectively, are consistent with a humid climate characterized by moderate to high rainfall. Although the estimated MAT of 17ºC for PQ5 should be treated with caution, given the uncertainty in analyses and calibration, it is broadly consistent with the mesothermal to megathermal climatic conditions inferred from palynological analyses.

A hot and wet climate is also consistent with the very high proportions of kaolinite. Clay minerals and associated minerals have been formed through weathering processes and pedogenesis through geological history, at least since the late Precambrian, and represent the most ubiquitous components of all sediments and soils. Clay mineral assemblages can be used to interpret paleoclimate, and specifically the intensity of weathering and by extension temperature and hydrological processes (Chamley, 1989; Millot, 1970). Interpretation is based on the variations of illite and chlorite crystallinity and on the relative abundance of kaolinite, smectite and other expandable minerals. According to Chamley, 1989, kaolinite is formed in soils and sediments of intertropical landmasses characterized by warm and humid climate. The weathering intensity is characterized by the monosiallitisation, a very intense weathering process. However, the absence of aluminium oxides such as gibbsite, indicate that the most intense weathering stage of allitisation (hot and wet in tropical areas) was not reached in the Krappfeld.

6.4 Comparison with the hyperthermal at the PETM?

In comparison with the slightly older microflora of St. Pankraz from the short-lived hyperthermal at the Paleocene/Eocene boundary (PETM-flora; Hofmann et al., 2011), the Krappfeld assemblages have no Paleogene elements and comprise far more palm taxa (17 versus two or three) and megathermal taxa (e.g., Malvaceae, Sapotaceae, *Alangium*) and much less diverse *Normapolles* s.l. and, Post-*Normapolles* taxa and less various extinct triporate forms (Juglandaceae, Myricaceae) and more Fagaceae in quantity but also in quality. However, a few megathermal accessory elements such as *Aiphanes*-type pollen (Arecoideae, Arecaceae), the *Aristogeitonia*-type pollen (Picrodendraceae), the *Iodes*-type pollen (Icacinaceae), the *Craigia*-type pollen (Tilioideae, Malvaceae), *Lannea*-type pollen (Anacardiaceae) and the *Palaquium*-type pollen (Sapotaceae) were already present during the PETM at St Pankraz. They were interpreted to have migrated west and northward along the Tethys during the already warm Paleogene (Hofmann, et al., 2011).

As other studies suggest that peak temperatures during the PETM were similar to or exceeded those of the EECO (Sluijs et al., 2011), the pollen data obtained here indicate that a longer time span was required for the “establishment” of a “real tropical” vegetation in the northwestern Tethys. During the relatively brief hyperthermals such as the PETM (Hofmann et al. 2011, Collinson et al., 2009) only a few megathermal elements reflected the warming.

In summary, the paleo-position of the Krappfeld in the northwestern Tethys (Fig. 3) provided enough air humidity, warmth and precipitation to support an ancient “subtropical to tropical flora” with an evergreen and deciduous forest, somewhat comparable to the zonoecotone I/II of today. This interpretation corroborates the observations from European Eocene macrofloras of Kvacek (2010), who postulated a “broad-leaved evergreen/semi-evergreen quasi-paratropical forest” for the western part and southwestern part (Tethyan realm) of Europe.

7. Conclusions

The black shale (sample PQ8) is interpreted as a coastal near transgessive deposit of the Krappfeld transgression during the biochrons NP11 and NP12. These biochrons indicate the section was deposited during the Early Eocene Climatic Optimum (Chron 24n). The Krappfeld terrestrial microflora represents a time period with warm and humid climatic conditions, and displays a higher degree of tropicality than the microflora of the PETM succession at St Pancraz. The composition of true megathermal, meso-to megathermal and temperate taxa and the high degree of taxa growing under seasonally controlled climatic conditions provides evidence for a seasonal controlled “subtropical to tropical” climate somewhat comparable with the modern zonoecotone I/II. The three different palynofacies are corroborated by biochemical biomarkers, which indicate peat forming environments under a pH condition common under warm and humid climates. The high amounts of kaolinite indicate intense weathering processes over a long period, also under warm and humid conditions that allowed the the main weathering product kaolinite to be reworked in high amounts into the basin. These humid conditions and reworking are also responsible for the dominance of terrestrial biomarkers even in the marine transgressive shale.

Acknowledgement

We thank Stjepan Coric for helping during fieldwork, Gerhard Hobiger for providing the Corg data, and Markus Kogler for preparing the line drawings.

References

Agnini, C., Marci, P., Backman, P., Brinkhuis, H., Fornaciari, E., Guisberti, L., Luciani, V., Rio, D., Sluijs, A. and Speranza, F., 2009. An early Eocene carbon cycle perturbation at – 52,5 Ma in the southern Alps: Chronology and biotic response. Paleoceanography 24, 2209.

Bijl, P.K., Schouten, S., Sluijs, A., Reichart, G.J., Zachos, J.C., and Brinkhuis, H. 2009. The early Palaeogene temperature evolution of the Southwest Pacific Ocean. Nature 461, 776-779.

Brindley, G.W. & Brown, G., 1980. Crystal Structures of Clay Minerals and their X-Ray Identification. Mineralogical Society, London, 495 pp..

Burnett, J.A. with contributions by Gallagher, L.T. and Hampton, N.G., 1998. Upper Cretaceous. In: P.R. Brown, (ed.), Calcareous Nannofossil Biostratigraphy. Chapman and Hall, Cambridge, 132-199.

Chamley, H., 1989. Clay Sedimentology. Springer Verlag, Berlin, 620 pp.

Cramer, B.S., Wright, J.D., Kent, D.V., Aubry, M.P., 2003. Orbital climate forcing of delta ^{13}C excursions in the late Paleocene-early Eocene (chrons 24n-25n). Paleoceanography 18, 1097.

Collinson, M.E., 1983. Fossil plants of the London Clay. The Palaeontological Association, London, 121pp.

Collinson, M.E., Steart, D.C., Harrington, G.J., Hooker, J.J., Scott, A.C., Allen, L.O., Glasspool, I.J. and Gibbons, S.J., 2009. Palynological evidence of vegetation dynamics in response to palaeoenvironmental change across the onset of the Palaeogene-Eocene Themal Maximum at Cobham, Southern England. Grana, 48, 38-66.

Dransfield, J., Uhl, N.W., Asmussen, C.B., Baker, W.J., Harley, M.M. and Lewis, C.E., 2008. Genera Palmarum – the evolution and classification of palm. Kew Publishing, Royal Botanical gardens, Kew, 737 pp.

Drobne, K., Egger, H., Hofmann, C., Mohamed, O., Ottner, F. and Rögl, F., 2011. Pemberger and Fuchsofen quarries to the west of Klein St. Paul. In: H. Egger, (ed), Climate and Biota of the Early Paleogene, Field-Trip Guidebook. Berichte der Geologischen Bundesanstalt, 86, 111-117.

Egger, H., Heilmann-Clausen, C. and Schmitz, B., 2009. From shelf to abyss: Record of the Palaeocene/Eocene-boundary in the Eastern Alps (Austria). Geologica Acta 7, 215-227.

Eglinton, G., Gonzalez, A.G., Hamilton, R.J. and Raphael, R. A., 1962. Hydrocarbonconstituents of the wax coatings of plant leaves - a taxanomic survey. Phytochemistry 1, 89-102.

Eglinton, G. and Hamilton, R.J., 1967. Leaf Epicuticular Waxes. Science 156, 1322-1335.

Ewel, K.C., 1992. Swamps. In: Meyers, R.L. and Ewel, J.J. (eds). Ecosystems of Florida. University of Central Florida Press, Orlando, 281-323.

Faegri, K. and Iversen, J., 1989. Textbook of pollen analysis, John Wiley and Sons, London, 328 pp.

Gentry, A.H., 1996. To the families and genera of woody plants of Northwest south America. University Chicago Press, 895 pp.

Galeotti, S., Krishan, S., Pagani, M., Lanci, L., Gaudio, A., Zachos, J.C., Monechi, S., Morelli, G. and Lourens, L., 2010. Orbital chronology of Early Eocene hyperthermals from the Contessa Road section, central Italy. Earth and Planetary Science Letters, 290, 192-200.

Gradstein, F.M., Ogg, J.O., Smith, A.G., Bleeker, W. and Lourens, L.J., 2004. A new Geologic time scale, with special reference to Precambrian and Neogene. Episodes 27, 83-100.

Hofmann, Ch.-Ch., 2002. Pollen distribution in sub-Recent sedimentary environments of the Orinoco Delta (Venezuela) – an actuo-palaeobotanical study. Review of Palaeobotany and Palynology, 119, 191-217.

Hofmann, Ch.-Ch. and Zetter, R., 2001. Palynological investigations of the Krappfeld area, Palaeocene/Eocene, Carinthia (Austria). Palaeontographica B, 259, 47-64.

Hofmann, Ch.-Ch. and Zetter, R. 2005. Reconstruction of different wetland plant habitats of the Pannonian basin system (Neogene, Eastern Austria). Palaios 20, 266-279.

Hofmann, Ch.-Ch., Zetter, R. and Draxler, I., 2002. Pollen- und Sporenvergesellschaftungen aus dem Karpatium des Korneuburger Beckens (Niederösterreich). Beiträge zur Paläontologie 17, 17-43.

Hofmann, Ch.-Ch., Mohamed, O. and Egger, H., 2011. A new terrestrial palynoflora from the Palaeocene/Eocene boundary in the northwestern Tethyan realm (St. Pankraz, Austria). Review of Paleobotany and Palynology 166, 295-310.

Hollis, J.C. and 11 others, 2009. Tropical sea temperatures in the high-latitude South Pacific during the Eocene. Geology, 37, 99-102.

Hopmans, E.C., Weijers, J.W.H., Schefuß, E., Herfort, L., Sinninghe Damsté, J.S. and Schouten, S., 2004. A novel proxy for terrestrial organic matter in sediments based on branched and isoprenoid tetraether lipids. Earth and Planetary Science Letters 224, 107-116.

Huber, M. and Caballero, R., 2011. The early Eocene equable climate problem revisited. Climates of the Past, Discussion, 7, 242-304.

Kennet, J.P. and Stott, L.D. 1991. Abrupt deep-sea warming, paleoceanographic changes and benthic extinctions at the end of the Paleocene. Nature 353, 225-229.

Kinter, E. B. & Diamond, S., 1956. A new Method for preparation and treatment of orientied - aggregate specimens of soil clays for X-Ray diffraction analysis. Soil Scince, 81, 111-120.

Klaus, W. 1987. Einführung in die Paläobotanik, Band 1. Deuticke Verlag, Wien, 314 pp.

Kolattukudy, P.E., 1976. The Chemistry and Biochemistry of Natural Waxes. Amsterdam, Elsevier.

Küchler, T. and Odin G.S., 2001. Upper Campanian-Maastrichtian ammonites (Nostoceratidae, Diplomoceratidae) from Tercis les Bains (Landes, France). Developments in Palaeontology and Stratigraphy, 19, 500-567.

Kvacek, S., 2910. Forest flora and vegetation of the European early Palaeogene – a review. Bulletin of Geosciences, 85, 63-76.

Lourens, L.J., Sluijs, A., Kroon; D.; Zachos; J.C., Thomas, E., Röhl, U., Bowles, J. and Raffi, I., 2005. Astronomical pacing of late Palaeocene to Eocene global warming events. Nature 435, 1083-1087.

Mabberly, D.J., 1992. Tropical rainforest ecology. Blackie London, 300 pp.

Mabberly, D.J., 2000. The Plant Book. Second edition. Cambridge University Press, Cambridge, 858 pp.

Mackenzie, R. C., 1964. The thermal investigation of soil clays. In: C.I. Rich and G.W. Kunze (eds.), Soil clay mineralogy ? A symposium. The University of North Carolina Press, Raleigh, North Carolina, 200-244.

Millot, G., 1970. Geology of clays. Springer Verlag, Berlin, 425 pp.

Moore, D.M. and Reynolds, R. C., Jr., 1997. X – Ray Diffraction and the Identification and Analysis of Clay Minerals. Oxford University Press, New York, 378 pp.

Muttoni, G. and Kent, D.V., 2007. Widespread formation of cherts during the early Eocene climate optimum. Palaeogeography, Palaeoclimatology, Palaeoecology, 253, 348-362.

Pancost, R. D., Baas, M., van Geel, B. and Sinninghe Damsté, J. S. 2003. Response of an ombrotrophic peat to a regional climatic event revealed by macrofossil, molecular, and carbon isotopic data. The Holocene 13, 921-932.

Pearson, P.N., van Dongen, B.E., Nicholas, C.J., Pancost, R. D., Schouten, S., Singano, J.M. and Wade, B.S. 2007. Stable warm tropical climate through the Eocene Epoch. Geology 35, 211-214.

Peters, K and Moldowan. J., 1991. Effects of source, thermal maturity, and biodegradation on the distribution and isomerisation of homohopanes in petroleum. Organic Geochemistry, 17, 47-61.

Peters. K, Walters, C. and Moldowan. J., 2005. The Biomarker Guide; Biomarkers and Isotopes in the Environment and Human History. Cambridge University Press, 1, Ed 2.

Reddi, C.S. and Reddi, N.S., 1986. Pollen production in some anemophilous angiosperms. Grana, 25, 55-61.

Riedmüller, G., 1978. Neoformations and Transformations of Clay Minerals in Tectonic Shear Zones. TMPM Tschermaks Mineralogische und Petrographische Mitteilungen 25, 219-242.

Röhl, U., Westerhold, T., Monechi, S., Thomas, E., Zachos, J.C. and Donner, B., 2005. The third and final early Eocene maximum: Characteristics, timing, and mechanisms of the “X” event. Annual Meeting of the Geological Society of America, Abstract, Salt Lake City.

Schaub, H., 1981. Nummulites et Assilines de la Tethys paleogene. Taxonomie, phylogenese et biostratigraphie. Schweizerische paläontologische Abhandlungen 104-106, 236 pp.

Schouten, S., Huguet, C., Hopmans, E. C., Kienhuis, M. V. M. and Sinninghe Damsté, J.S., 2007. Analytical methodology for TEX86 paleothermometry by high-performance liquid chromatography/atmospheric pressure chemical ionization-mass spectrometry. Analytical Chemistry, 79, 2940-2944.

Schultz, L. G., 1964. Quantitative Interpretation of Mineralogical Composition from X-Ray and Chemical Data of the Pierre Shales. U.S. Geological Survey Professional Paper, 391C, 1-31.

Sissingh, W. 1977. Biostratigraphy of Cretaceous calcareous nannoplankton. Geologie en Mijnbouw 56, 37-67.

Serra-Kiel, J., Hottinger, L., Caus, E., Drobne, K., Ferrandez, C., Jaurhi, A.K., Less, G., Pavlovec, R., Pignatti, J., Samso, J.M., Schaub, H., Sirel, E., Strougo, A., Tambareau, Y., Tosquella, J., Zakrevskaya, E., 1998. Larger foraminiferal biostratigraphy of the Tethyan Paleocene and Eocene. Société Géologique de France Bulletin, 169, 281-299.

Sluijs, A., Bijl, P.K., Röhl, U., Reichart, G.J. and Brinkhuis, H., 2011. Southern ocean warming, sea level and hydrological change during the Palaeocene-Eocene thermal maximum. Climates of the Past, 7, 47-61.

Smith, M.E., Singer, B., Carrol, A. 2003. 40Ar/39Ar geochronology of the Eocene Green River Basin. Geological Society of America Bulletin 115, 549-565.

Soliman, A., Suttner, T.J., Lukeneder, A., Summesberger, H., 2009. Dinoflagellate cysts and Ammonoids from Upper Cretaceous sediments of the Pemberger Formation (Krappfeld, Carinthia, Austria). Annalen des Naturhistorisches Museum Wien, 110A, 401-421.

Stampfli, G.M., Mosar, J., Marquer, D., Marchant, R., Baudin, T., Borel, G., 1998. Subduction and obduction processes in the Swiss Alps. Tectonophysics, 296, 159-204.

Stap, L., Lourens, L. J., Thomas, E., Slujis, A., Bohaty, S., Zachos, J.C., 2010. High-resolution deep-sea carbon and oxygen isotope records of Eocene Thermal Maximum 2 and H2. Geology, 38, 607-610.

Thiedig, F. and Wiedmann, J., 1976. Ammoniten und Alter der höheren Kreide (Gosau) des Krappfeldes in Kärnten (Österreich). Mitteilungen des Geologisch-Paläontologischen Instituts der Universität Hamburg, 45, 9-27.

Thiedig, F.,. v. Husen, D. and Pistotnik, J., 1999. Geologische Karte Österreich 1:50000, Blatt 186 St. Veit an der Glan. Geologische Bundesanstalt, Wien.

Thorez, J.,1975. Phyllosilicates and clay minerals - a laboratory handbook for their x-ray diffraction analysis. Editions G. Lelotte, Liege, 579 pp.

Tributh, H.,1989. Notwendigkeit und Vorteil der Aufbereitung von Boden- und Lagerstättentonen. In: H. Tributh and G Lagaly (eds.), Identifizierung und Charakterisierung von Tonmineralen, 29-33, Giessen.

Vandenberghe, N., van Simaeys, S., Steurbaut, E., Jagt, J.W. M., and Felder, P.J., 2004. Stratigraphic architecture of the Upper Cretaceous and Cenozoic along the southern border of the North Sea basin in berlgium. Netherlands Journal of Geosciences 83, 155-171.

van Hillebrandt, A.,1993. Nummuliten und Assilinen aus dem Eozän des Krappfeldes in Kärnten (Österreich). Zitteliana 20, 277-293.

Vanhove, D. Stassen, P., Speijer, R.P. and Steurbaut, E. 2011. Assessing palaeotemperature and seasonality during the early Eocene climatic optimum (EECO) in the Belgian Basin by means of fish otolith stable isotopes. Geologica Belgica, 14, 143-158.

Vareschi, V. 1980. Vegetationsökologie der Tropen. Eugen Ulmer Verlag, Stuttgart, 293 pp.

Wagreich, M. 1993. Subcrustal tectonic erosion in orogenic belts - A model for the Late Cretaceous subsidence of the Northern Calcareous Alps (Austria). Geology, 21, 941-944.

Wagreich, M. (2001). Paleocene - Eocene paleogeography of the Northern Calcareous Alps (Gosau Group, Austria). In: W.E. Piller and M.W. Rasser (eds.), Paleogene of the Eastern Alps. Österreichische Akademie der Wissenschaften, Schriftenreihe der Erdwissenschaftlichen Kommissionen, 14, 57-75.

Walter, H. and Breckle, S.W., 1999. Vegetation und Klimazonen. Verlag Eugen Ulmer Stuttgart, 544 pp.

Westerhold, T., Röhl, U., Laskar, J., Raffi, I., Bowles, J., Lourens, L. and Zachos, J.C., 2007. On the duration of magnetochrons C24r and C25n and the timing of the early Eocene global warming events: Implications from the Ocean Drilling Program Leg 208 Walvis Ridge depth transect. Paleoceanography, 22 PA2201, doi:10.1029/2006PA001322.

Wignall, P.B., 1994. Black Shales. Oxford Monographs on Geology and Geophysics (Clarendon Press, Oxford), 127 pp.

Wilkens, E., 1985. Das Alttertiär des Krappfeldes (Kärnten, Österreich). Unpubl. Diploma thesis, University of Hamburg, 195 pp.

Wilson, M.J., 1987. A handbook of determinative methods in clay mineralogy. Verlag Blackie, Glasgow and London, 308 pp.

Whitmore, T.C., 1992. An Introduction to tropical rain forests. Clarendon, Oxford, 226 pp.

Whittig, L.D., 1965. X-ray diffraction techniques for mineral identification and mineralogical identification. In: C.A. Black (ed.), Methods of Soil Analysis. American Society of Agronomy., Madison, Wisconsin, pp. 671-698.

Zachos, J., Pagani, M., Sloan, L., Thomas, E. and Billups, K., 2001. Trends, rhythms, and aberrations in global climate 65 Ma to present. Science 292, 686-693.

Zachos, J.C., Dickens, G.R. Zeebe, R.E., 2008. An early Cenozoic perspective on greenhouse warming and carbon-cycle dynamics. Nature, 451, 279-283.

Zachos, J.C., Mc Carren, H., Murphy, B., Röhl, U. and Westerhold, T., 2010. Tempo and scale of late Paleocene and early Eocene isotope cycles: Implication fort he origin of hyperthermals. Earth and Planetary Science Letters 299, 242-249.

Zetter, R. and Hofmann, Ch.-Ch., 2001. New aspects of the palynoflora of the lowermost Eocene (Krappfeld, Carinthia). Österreische Akademie der Wissenschaften, Schriftenreihe der Erdwissenschaftlichen Kommission, 14, 473-507.

Received: 30 November 2011
Accepted: 16 March 2012

Christa-Ch. HOFMANN[1)*], Richard PANCOST[2)], Franz OTTNER[3)], Hans EGGER[4)], Kyle TAYLOR[2)], Omar MOHAMED[5)] & Reinhard ZETTER[1)]

[1)] University of Vienna, Department of Palaeontology, Althanstr. 14, 1090 Vienna, Austria;

[2)] Organic Geochemistry Unit, Bristol Biogeochemistry Research Centre and The Cabot Institute, School of Chemistry, University of Bristol, Cantock's Close, BS8 1TS Bristol, UK;

[3)] University of Natural Resources and Applied Life Sciences, Gregor Mendel Straße 33, 1090 Vienna, Austria;

[4)] Geological Survey of Austria, Neulinggasse 38, 1030 Vienna, Austria;

[5)] El Minia University, Department of Geology, El Minia, Egypt;

[*)] Corresponding author, christa.hofmann@univie.ac.at

Plate 1:

Megathermal elements:

Figure A-C: *Spinizonocolpites* sp. (Arecaceae, Nypoideae, *Nypa* = mangrove palm)

Figure D-F: *Dicolpopollis* sp. (Arecaceae, Calamoideae, *Calamus* = rattan palm)

Figure G-I: *Monocolpopollenites* sp. (Arecaceae, Coccosae, *Elais*-type = oil palm)

Figure J-L: *Alangiopollis* sp. (*Alangiaceae*, *Alangium villosum*-type)

Figure M-O: *Anacolosites* sp. (Olacaceae, *Anacolosa*-type)

Magnifications: A x 800, D, G, I & M x 1000; bars in B, E, H, K & N = 10µm, bars in C, F, I, L & O = 2µm.

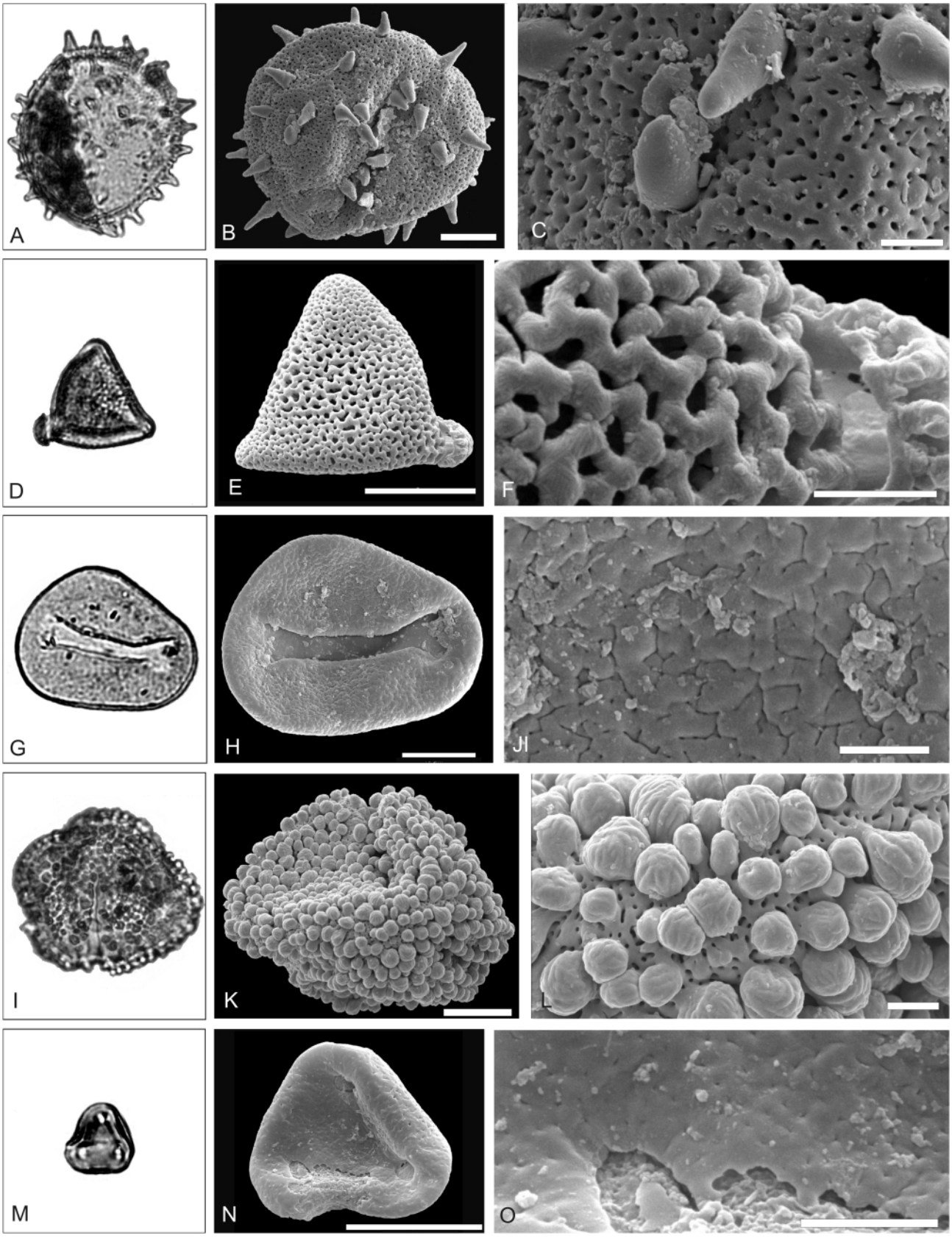
A
B
C
D
E
F
G
H
JI
I
K
L
M
N
O

Plate 2:

Seasonal controlled meso- to megathermal elements:

Figure A-C: Thymeleaceae (*Wikstroemia*-type)

Figure D-F: Avicenniaceae (*Avicennia*-type, black mangrove)

Figure G-I: Hamamelidaceae (*Corylopsis*-type)

Figure J-L: *Malvacipollis* sp. (Picrodendraceae, *Aristogeitonia*-type)

Figure M-O: Euphorbiaceae (*Leucroton*-type)

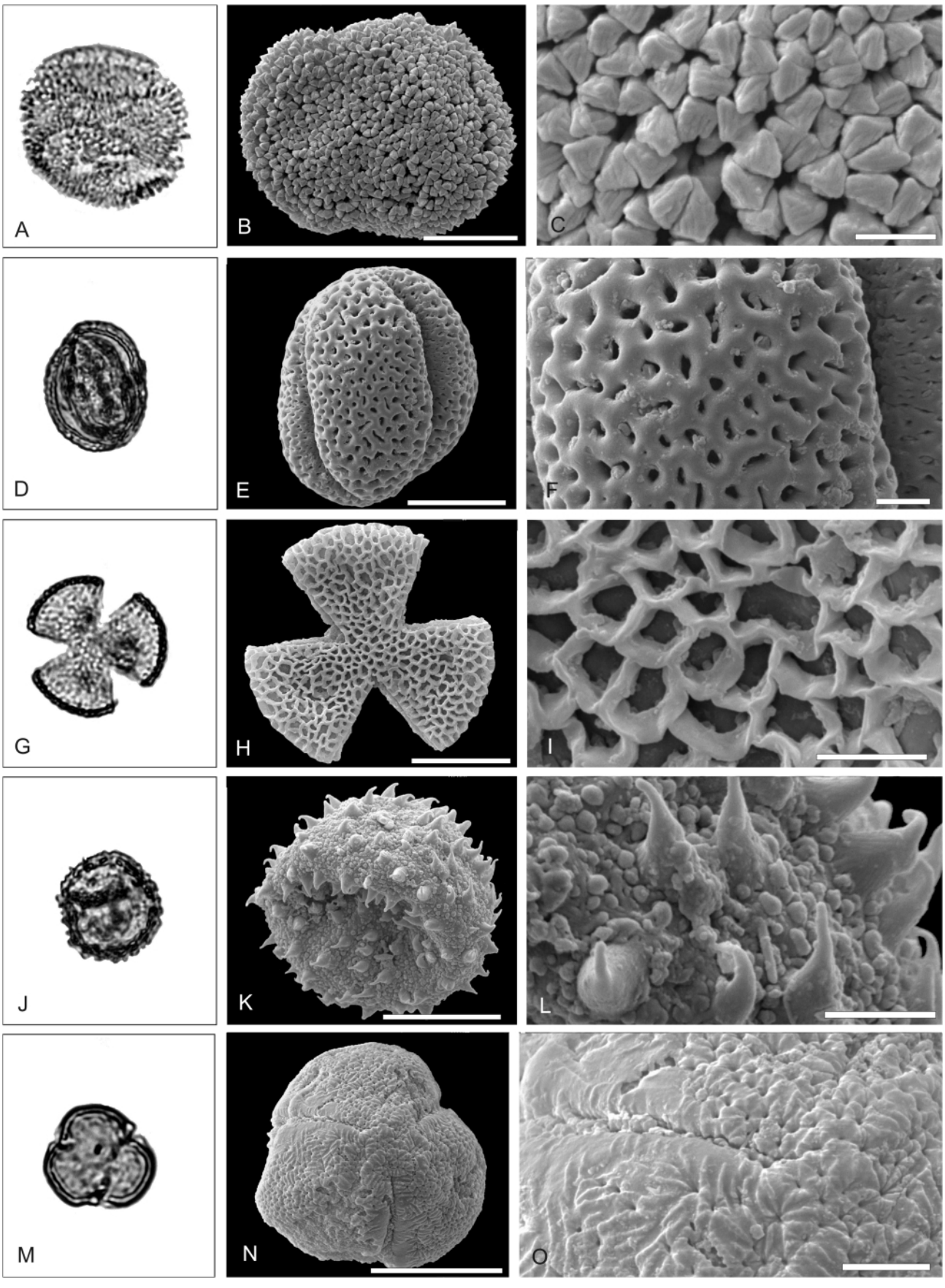
A
B
C
D
E
F
G
H
I
J
K
L
M
N
O